

## The Origin of Stark Splitting in the Initial Photoproduct State of MbCO

Karin Nienhaus,<sup>‡</sup> John S. Olson,<sup>§</sup> Stefan Franzen,<sup>⊥</sup> and G. Ulrich Nienhaus<sup>\*,‡,||</sup>

University of Ulm, Department of Biophysics, Albert-Einstein-Allee 11, 89081 Ulm, Germany, Rice University, Department of Biochemistry and Cell Biology and the W. M. Keck Center of Computational Biology, Houston, Texas 77005-1892, North Carolina State University, Department of Chemistry, Raleigh, North Carolina 27695, and University of Illinois at Urbana-Champaign, Department of Physics, 1110 West Green Street, Urbana, Illinois 61801

Received June 5, 2004; E-mail: uli@uiuc.edu

A microscopic structural description of the deceptively simple process of ligand photodissociation and recombination in myoglobin (Mb) has begun to emerge with the application of low-temperature<sup>1–5</sup> and time-resolved<sup>6–9</sup> X-ray crystallography. Within picoseconds after photolysis, the ligand settles into an initial docking site B<sup>10</sup> on top of the heme group, parallel to pyrrole C,<sup>1–10</sup> where it resides for several nanoseconds before either rebinding or escaping. Electron density maps of the initial B state photoproduct reveal only a single location for the dissociated CO, whereas two major spectrally and kinetically distinct states, B<sub>1</sub> and B<sub>2</sub>, are observed in time-resolved and low-temperature infrared spectra.<sup>10–14</sup> Lim et al.<sup>10</sup> proposed that the CO molecule adopts two opposite orientations in these states. They assigned the high frequency (~2130 cm<sup>-1</sup>) B<sub>1</sub> state to the conformer with the O atom pointing back toward the heme iron atom and the low frequency (~2120 cm<sup>-1</sup>) B<sub>2</sub> state to the other orientation, on the basis of the kinetics of the appearance of the  $\nu_{\text{CO}}$  bands after photolysis and the effects of isotopic substitution on the rate of recombination.<sup>14</sup> Recently, we have made the opposite assignments on the basis of mutagenesis data.<sup>15</sup>

In view of this discrepancy, we have reexamined the effects of mutating His64 and Val68 on the CO infrared stretching bands associated with the B<sub>1</sub> and B<sub>2</sub> photoproduct states. Wild-type, H64L, V68F, and H64L–V68F MbCO were selected for experimental and theoretical analyses. Fourier transform infrared (FTIR) spectroscopy and density functional theory (DFT) calculations were combined to examine the effects of the electrostatic environment on the B state photoproduct bands.

Free CO gas<sup>16</sup> absorbs at 2143 cm<sup>-1</sup>. Within the protein matrix, the stretching frequencies  $\nu_{\text{CO}}$  of both heme-bound and dissociated CO are shifted by the internal electric field acting on the CO dipole.<sup>17–22</sup> Hydrogen bonding between the CO and a donor side chain can be considered equivalent to an externally applied electric field, with the X–H dipole (X = N, O, C) causing the Stark shifts.<sup>19</sup> The C–O bond length is altered by electrical and mechanical anharmonic interactions with the dipole moment of the X–H group.<sup>31</sup> Quantitative models of the  $\nu_{\text{CO}}$  shifts of heme-bound CO in many MbCO mutants indicate a significant effect of hydrogen bonding on  $\nu_{\text{CO}}$ .<sup>19</sup> Using similar models, we have studied the interactions that cause the observed splitting of the B state bands and have related CO orientation with  $\nu_{\text{CO}}$ .

At neutral pH, wild-type and V68F MbCO display similar heme-bound CO spectra, with contributions from bound states A<sub>1</sub> and A<sub>3</sub> (Figure 1a).<sup>15,23</sup> In the absence of the distal histidine (H64L and H64L–V68F MbCO), a single A<sub>0</sub> band is visible. After photolysis of wild-type MbCO at 3 K,<sup>13</sup> the major B<sub>1</sub> and B<sub>2</sub>

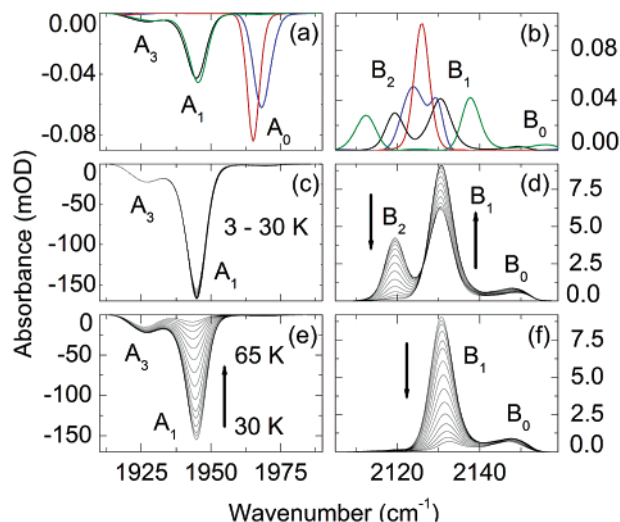


**Figure 1.** (a, b) FTIR photolysis difference spectra of wild-type MbCO (black) and mutants H64L (red), V68F (green), and H64L–V68F (blue), calculated from transmission spectra collected before and after 1-s illumination at 3 K (pH 7.5, areas normalized to 1 OD cm<sup>-1</sup>). FTIR spectra of wild-type MbCO during a temperature ramp (5 mK/s) from (c, d) 3–30 K and (e, f) 30–65 K.

photoproduct bands are at 2131 and 2119 cm<sup>-1</sup>. The small B<sub>0</sub> population at 2149 cm<sup>-1</sup> is associated with the minor A<sub>3</sub> state.<sup>24</sup> The Stark splitting between B<sub>1</sub> and B<sub>2</sub> increases from H64L < H64L–V68F < wild-type < V68F Mb (Figure 1b).

After photolysis at 3 K and slow heating (5 mK/s) to 30 K, very little CO rebinds to Mb, as judged from the small change in spectral area (Figure 1c). However, there is a net conversion from the B<sub>2</sub> to the B<sub>1</sub> conformer (Figure 1d). The barrier against this exchange is small (3–4 kJ/mol)<sup>13</sup> compared to that against recombination at the heme iron, ~10 kJ/mol.<sup>11</sup> The B<sub>2</sub> to B<sub>1</sub> transition appears to involve a simple rotation of the ligand about the center of the C–O bond. Warming to ~50 K causes the B<sub>1</sub> peak to disappear with concomitant reformation of the A<sub>1</sub> state (Figure 1 e, f). Thus, rebinding occurs primarily from B<sub>1</sub>.

Here we propose that the ligand carbon is directed toward the heme iron in B<sub>1</sub> (Figure 2). Both theory and experiment support the presence of the N<sub>e</sub>–H tautomer of His64 in the A<sub>1</sub> and A<sub>3</sub> states.<sup>19,21,25,26</sup> Upon photodissociation at 3 K, a change to the N<sub>δ</sub>–H tautomer is unlikely to occur in the frozen protein. Consequently, our assignment implies a direct hydrogen bonding interaction between the N<sub>e</sub>–H atom of His64 and the CO ligand. The N<sub>e</sub>–H...C–O interaction should increase the bond order and  $\nu_{\text{CO}}$  of unbound CO, whereas the N–H...O–C interaction should decrease both. In H64L MbCO, the Stark splitting is absent, although both CO orientations are likely to occur in the photoproduct (Figure 1b).

<sup>‡</sup> University of Ulm.<sup>§</sup> Rice University.<sup>⊥</sup> North Carolina State University.<sup>||</sup> University of Illinois at Urbana-Champaign.

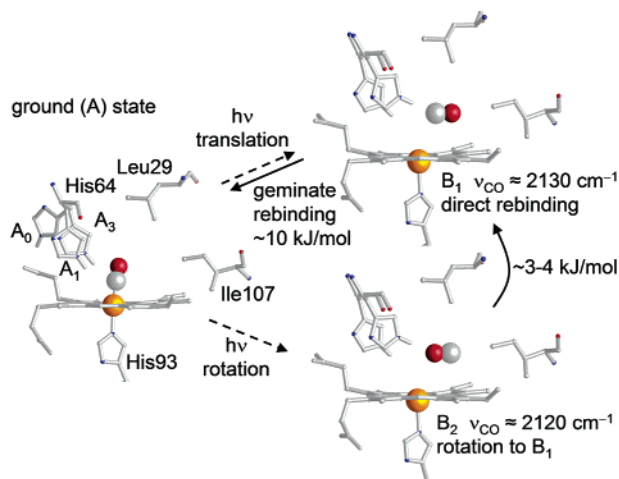


**Figure 2.** (Left) Schematic representation of heme-bound states  $A_0$ ,  $A_1$ , and  $A_3$ . The O and C atoms of the ligand are red and white, respectively. (Right) Photoproduct states  $B_1$  and  $B_2$ , with the His64 imidazole farther away from dissociated ligand, as in the 40 K Mb\*CO photoproduct (PDB code 1ABS), and closer, as in deoxyMb (PDB code 2MGL), and most electron density maps of photodissociated MbCO at room temperature.<sup>1,7</sup>

**Table 1.** Infrared Bands of the Initial Photoproduct of MbCO

sample/model	$\nu_{CO} (\text{cm}^{-1})$		
	$B_2$	$B_1$	$B_0$
wild-type MbCO (exp)	2119 (37) <sup>a</sup>	2131 (58)	2149 (5)
Im-H $\cdots$ OC, CO (porph.)	2122	2129	
H64L (exp)		2126 (100)	
H64L-V68F (exp)	2124 (28)	2130 (72)	
V68F (exp)	2112 (39)	2138 (53)	2156 (8)

<sup>a</sup> In parentheses: percentage of the total absorbance.

This observation suggests strongly that proton donation by His64 plays a predominant role in the wild-type protein. The V68F mutation enhances the Stark splitting significantly (Figure 1b, Table 1). The large benzyl side chain fills the back of the distal pocket, sequesters the photodissociated CO closer to the His64 side chain, and provides an additional electrostatic field.<sup>15,27</sup> The latter effect of the phenyl ring can be seen in the H64L-V68F double mutant as a small splitting of the B state peaks ( $\sim 6 \text{ cm}^{-1}$ , Figure 1 and Table 1).

To test the feasibility of the proposed  $B_1$  and  $B_2$  assignment, calculations of the expected vibrational frequencies of photodissociated CO were carried out on a series of simple model systems using DFT methods (DMol3, Accelrys, Inc.).<sup>19,28–31</sup> Stretching frequencies at 2158 and  $2152 \text{ cm}^{-1}$  are obtained for single hydrogen-bonding interactions in Im-N $\epsilon$ -H $\cdots$ CO and Im-N $\epsilon$ -H $\cdots$ OC (N $\epsilon$  $\cdots$ ligand distance: 3.5 Å). Earlier studies have indicated marked contributions from the porphyrin ring and other side chains in the distal pocket.<sup>32,33</sup> More complex, energy-minimized Im-H $\cdots$ CO $\cdots$ H-CH $_3$  and Im-H $\cdots$ OC $\cdots$ H-CH $_3$  models including two interactions predict stretching frequencies of 2179 and  $2151 \text{ cm}^{-1}$ , where the methane molecule mimics the interaction of the CO with the methyl groups of Leu29 or Ile107 (Figure 2). When the CO was placed above a simple porphine macrocycle as a more realistic model, the  $\nu_{CO}$  values of Im-H $\cdots$ CO and Im-H $\cdots$ OC were calculated to be 2129 and  $2122 \text{ cm}^{-1}$  (Table 1, Supporting Information).

The relative frequency shifts for all the models are in agreement with the assignments of the experimentally observed  $B_1$  and  $B_2$  bands in Figure 2, although the magnitudes vary. Our interpretation of the B states is also consistent with DFT estimates of the energies of Im-H $\cdots$ CO versus Im-H $\cdots$ OC interactions which show that

hydrogen-bond donation to the C atom produces a  $\sim 7 \text{ kJ/mol}$  lower energy state than the alternative orientation, accounting for the  $B_2$  to  $B_1$  interconversion between 3 and 30 K (Figure 1d).

**Acknowledgment.** G.U.N. is supported by grants from the DFG (Ni-291/3) and the Fonds der Chemischen Industrie. J.S.O. is supported by NIH Grants GM 35649 and HL 47020 and the Robert A. Welch Foundation Grant C-612. S. F. thanks the NSF for support through Grant MCB-9874895.

**Supporting Information Available:** Stretching frequencies and bond lengths obtained from DFT calculations of selected model systems, including coordinates. This material is available free of charge via the Internet at <http://pubs.acs.org>.

## References

- (1) Teng, T. Y.; Srajer, V.; Moffat, K. *Nat. Struct. Biol.* **1994**, *1*, 701–705.
- (2) Schlichting, I.; Berendzen, J.; Phillips, G. N., Jr.; Sweet, R. M. *Nature* **1994**, *371*, 808–812.
- (3) Hartmann, H.; Zinser, S.; Komminos, P.; Schneider, R. T.; Nienhaus, G. U.; Parak, F. *Proc. Natl. Acad. Sci. U.S.A.* **1996**, *93*, 7013–7016.
- (4) Ostermann, A.; Waschipky, R.; Parak, F. G.; Nienhaus, G. U. *Nature* **2000**, *404*, 205–208.
- (5) Chu, K.; Vojtechovsky, J.; McMahon, B. H.; Sweet, R. M.; Berendzen, J.; Schlichting, I. *Nature* **2000**, *403*, 921–923.
- (6) Srajer, V.; Teng, T.; Ursby, T.; Pradervand, C.; Ren, Z.; Adachi, S.; Schildkamp, W.; Bourgeois, D.; Wulff, M.; Moffat, K. *Science* **1996**, *274*, 1726–1729.
- (7) Schotte, F.; Lim, M.; Jackson, T. A.; Smirnov, A. V.; Soman, J.; Olson, J. S.; Phillips, G. N., Jr.; Wulff, M.; Anfinrud, P. A. *Science* **2003**, *300*, 1944–1947.
- (8) Bourgeois, D.; Vallone, B.; Schotte, F.; Arcovito, A.; Miele, A. E.; Sciarra, G.; Wulff, M.; Anfinrud, P.; Brunori, M. *Proc. Natl. Acad. Sci. U.S.A.* **2003**, *100*, 8704–8709.
- (9) Srajer, V.; Ren, Z.; Teng, T. Y.; Schmidt, M.; Ursby, T.; Bourgeois, D.; Pradervand, C.; Schildkamp, W.; Wulff, M.; Moffat, K. *Biochemistry* **2001**, *40*, 13802–13815.
- (10) Lim, M.; Jackson, T. A.; Anfinrud, P. A. *Nat. Struct. Biol.* **1997**, *4*, 209–214.
- (11) Nienhaus, G. U.; Mourant, J. R.; Chu, K.; Frauenfelder, H. *Biochemistry* **1994**, *33*, 13413–13430.
- (12) Nienhaus, K.; Deng, P.; Kriegl, J. M.; Nienhaus, G. U. *Biochemistry* **2003**, *42*, 9647–9658.
- (13) Frauenfelder, H.; Good, D.; McDonald, J. D.; Marden, M. C.; Moh, P. P.; Reinisch, L.; Reynolds, A. H.; Shyamsunder, E.; Yue, K. T. *Proc. Natl. Acad. Sci. U.S.A.* **1982**, *79*, 3744–3748.
- (14) Alben, J. O.; Beece, D.; Bowne, S. F.; Eisenstein, L.; Frauenfelder, H.; Good, D.; Marden, M.; Moh, P. P.; Reinisch, L.; Reynolds, A. H.; Yue, K. T. *Phys. Rev. Lett.* **1980**, *44*, 1157–1160.
- (15) Nienhaus, K.; Deng, P.; Olson, J. S.; Warren, J. J.; Nienhaus, G. U. *J. Biol. Chem.* **2003**, *278*, 42532–42544.
- (16) Ewing, G. E. *J. Chem. Phys.* **1962**, *37*, 2250–2256.
- (17) Park, E. S.; Andrews, S. S.; Hu, R. B.; Boxer, S. G. *J. Phys. Chem. B* **1999**, *103*, 9813–9817.
- (18) Park, E. S.; Thomas, M. R.; Boxer, S. G. *J. Am. Chem. Soc.* **2000**, *122*, 12997–12303.
- (19) Franzen, S. *J. Am. Chem. Soc.* **2002**, *124*, 13271–13281.
- (20) Ray, G. B.; Li, X.-Y.; Ibers, J. A.; Sessler, J. L.; Spiro, G. S. *J. Am. Chem. Soc.* **1994**, *116*, 162–176.
- (21) Phillips, G. N., Jr.; Teodoro, M. L.; Li, T.; Smith, B.; Olson, J. S. *J. Phys. Chem. B* **1999**, *103*, 8817–8829.
- (22) Kriegl, J. M.; Nienhaus, K.; Deng, P.; Fuchs, J.; Nienhaus, G. U. *Proc. Natl. Acad. Sci. U.S.A.* **2003**, *100*, 7069–7074.
- (23) Vojtechovsky, J.; Chu, K.; Berendzen, J.; Sweet, R. M.; Schlichting, I. *Biophys. J.* **1999**, *77*, 2153–2174.
- (24) Mourant, J. R.; Braunstein, D. P.; Chu, K.; Frauenfelder, H.; Nienhaus, G. U.; Ormos, P.; Young, R. D. *Biophys. J.* **1993**, *65*, 1496–1507.
- (25) Merchant, K. A.; Noid, W. G.; Akiyama, R.; Finkelstein, I. J.; Goun, A.; McClain, B. L.; Loring, R. F.; Fayer, M. D. *J. Am. Chem. Soc.* **2003**, *125*, 13804–13818.
- (26) Sagnella, D. E.; Straub, J. E. *Biophys. J.* **1999**, *77*, 70–84.
- (27) Quillin, M. L.; Li, T.; Olson, J. S.; Phillips, G. N., Jr.; Dou, Y.; Ikeda-Saito, M.; Regan, R.; Carlson, M.; Gibson, Q. H.; Li, H.; Elber, R. J. *Mol. Biol.* **1995**, *245*, 416–436.
- (28) Delley, B. *J. Chem. Phys.* **1990**, *92*, 508–517.
- (29) Delley, B. *J. Chem. Phys.* **2000**, *113*, 7756–7764.
- (30) Perdew, J. P.; Chevary, J. A.; Vosko, S. H.; Jackson, K. A.; Pederson, M. R.; Singh, D. J.; Fiolhais, C. *Phys. Rev. B* **1992**, *46*, 6671–6687.
- (31) Brewer, S. H.; Franzen, S. *J. Chem. Phys.* **2003**, *119*, 851–858.
- (32) Nutt, D. R.; Meuwly, M. *Biophys. J.* **2003**, *85*, 3612–3623.
- (33) McMahon, B. H.; Stojkovic, B. P.; Hay, P. J.; Martin, R. L.; García, A. E. *J. Chem. Phys.* **2000**, *113*, 6831–6850.

JA0466917